

Anion type-dependent confinement effect on glass transitions of solutions of LiTFSI and LiFSI

Jinbing Zhang(张晋兵), Fengping Wang(王凤平), Zexian Cao(曹则贤), and Qiang Wang(王强)
Citation: Chin. Phys. B, 2023, 32 (**7**): 076401. DOI: 10.1088/1674-1056/acca0d
Journal homepage: http://cpb.iphy.ac.cn; http://iopscience.iop.org/cpb

What follows is a list of articles you may be interested in

Internal friction behavior of $Zr_{59}Fe_{18}Al_{10}Ni_{10}Nb_3$ metallic glass under different aging temperatures

Israa Faisal Ghazi, Israa Meften Hashim, Aravindhan Surendar, Nalbiy Salikhovich Tuguz, Aseel M. Aljeboree, Ayad F. Alkaim, and Nisith Geetha
Chin. Phys. B, 2021, 30 (**2**): 026401. DOI: 10.1088/1674-1056/abc14f

Thermal effects and evolution of the defect concentration based on shear modulus relaxation data in a Zr-based metallic glass

Qi Hao(郝奇), Ji-Chao Qiao(乔吉超), E V Goncharova, G V Afonin, Min-Na Liu(刘敏娜), Yi-Ting Cheng(程怡婷), V A Khonik
Chin. Phys. B, 2020, 29 (**8**): 086402. DOI: 10.1088/1674-1056/ab969c

Secondary relaxation and dynamic heterogeneity in metallic glasses: A brief review

J C Qiao(乔吉超), Q Wang, D Crespo, Y Yang(杨勇), J M Pelletier
Chin. Phys. B, 2017, 26 (**1**): 016402. DOI: 10.1088/1674-1056/26/1/016402

Decline of nucleation in the heating process with a high heating rate

Yang Gao-Lin (杨高林), Lin Xin (林鑫), Song Meng-Hua (宋梦华), Hu Qiao (胡桥), Wang Zhi-Tai (汪志太), Huang Wei-Dong (黄卫东)
Chin. Phys. B, 2014, 23 (**8**): 086401. DOI: 10.1088/1674-1056/23/8/086401

Liquid to glass transition of tetrahydrofuran and 2-methyltetrahydrofuran

Tan Rong-Ri (谈荣日), Shen Xin (沈鑫), Hu Lin (胡林), Zhang Feng-Shou (张丰收)
Chin. Phys. B, 2012, 21 (**8**): 086402. DOI: 10.1088/1674-1056/21/8/086402

Anion type-dependent confinement effect on glass transitions of solutions of LiTFSI and LiFSI

Jinbing Zhang(张晋兵)[1,2], Fengping Wang(王凤平)[1,†], Zexian Cao(曹则贤)[2,3], and Qiang Wang(王强)[2,‡]

[1] *School of Mathematics and Physics, University of Science and Technology Beijing, Beijing* 100083, *China*
[2] *Beijing National Laboratory for Condensed Matter Physics, Institute of Physics, Chinese Academy of Sciences, Beijing* 100190, *China*
[3] *Songshan Lake Materials Laboratory, Dongguan* 523808, *China*

(Received 3 March 2023; revised manuscript received 4 April 2023; accepted manuscript online 4 April 2023)

We present findings on the effect of nanometer-sized silica-based pores on the glass transition of aqueous solutions of lithium bis(trifluoromethane)sulfonimide (LiTFSI) and lithium difluorosulfimide (LiFSI), respectively. Our experimental results demonstrate a clear dependence of the confinement effect on the anion type, particularly for water-rich solutions, in which the precipitation of crystalized ice under cooling process induces the formation of freeze-concentrated phase confined between pore wall and core ice. As this liquid layer becomes thinner, the freeze-concentrated phase experiences glass transition at increasingly higher temperatures in solutions of LiTFSI. However, differently, for solutions of LiFSI and LiCl, this secondary confinement has a negligible effect on the glass transition of solutions confined wherein. These different behaviors emphasize the obvious difference in the dynamic properties' response of LiTFSI and LiFSI solutions to spatial confinement and particularly to the presence of the hydrophilic pore wall.

Keywords: anion type-dependent confinement effect, glass transition, Li salts, aqueous solutions

PACS: 64.70.P–, 61.43.Gt, 68.15.+e, 78.55.Qr **DOI:** 10.1088/1674-1056/acca0d

1. Introduction

The electrolytes of lithium salt are widely used in batteries and large energy storage devices, making them crucial in daily life and industrial production.[1–8] Current research has focused on the ionic conductivity, structural heterogeneity, and interaction between the electrolyte and solid surface which leads to the formation of a solid-electrolyte-interphase in bulk aqueous solutions of lithium salts. Recently, Peng and Ye *et al.*[9] discovered that 21-mol/kg LiTFSI solution confined in two-dimensional (2D) graphene oxide (GO) nanochannels demonstrated a quadrupled ionic conductivity in comparison to bulk solutions. This observation suggests that a layered structure is formed within the confinement condition, where a free anion layer moves between two continuous water-cation layers, resulting in a significant increase in ionic transport. Additionally, Chava *et al.*[10] have proposed, based on molecular dynamics (MD) simulation, that solutions of LiTFSI confined within boron nitride nanotube with a diameter of 1 nanometer show the dehydration of some $TFSI^-$ anions in 5-mol/kg and 10-mol/kg LiTFSI solutions, leading to the localization of the cation–anion pair at the negative electrode. A crucial observation is that the concentration required for dehydration of the anions within the confined solution is significantly lower compared to that required for bulk solutions. This highlights the strong influence of confinement conditions on the interactions between the anion, cation, and solvent such as water, owing to size and/or interface effects. Moreover, the effect of solution–channel/pore surface interactions was particularly investigated by Li *et al.*[11] They have demonstrated how a surface potential-induced interfacial electrical double layer, along with nano-confinement, can manipulate ion diffusion for KCl solutions confined in charged layered graphene-based nano-porous membranes. Additionally, Pham and coworkers,[12] using a combination of first-principles and classical MD simulations, investigated the effects of water polarization and cation-π interactions on the ion solvation, particularly for large ions with weak hydration energies in carbon nanotubes with a diameter of 1 nm–2 nm. These results highlight how confinement alters the interactions among the anion, cation, and water, which may not be easily discernible in bulk systems.

This study explores the effect of spatial confinement on the dynamic properties of LiTFSI solution, specifically the concentration-dependent glass transition in nano-pores. The behavior of the glass transition under spatial confinement actually has been extensively investigated. One objective is to understand the structural and dynamic inhomogeneity in deeply supercooled glass-forming liquids.[13–25] It is reasonable to propose that the size of the spatial constraint should be the upper limit of the heterogeneous domains of glass forming liquids.[23,26] Hence, when it comes to confinement, it is expected that nanometer-sized pores or channels, especially with diameters less than 2 nm, will reduce the glass transition temperature T_g of confined liquids, as compared to the T_g of bulk

†Corresponding author. E-mail: fpwang@ustb.edu.cn
‡Corresponding author. E-mail: qwang@iphy.ac.cn

© 2023 Chinese Physical Society and IOP Publishing Ltd

liquids. However, conversely, the interaction of the liquid with the pore walls may cause an increase in T_g. These two factors induced vitrification of eutectic NaCl solution[16] as well as relatively diluted LiCl solutions.[19] These solutions only undergo total vitrification under high pressures when in their bulk states.

This study emphasizes the distinctive dynamic behaviors displayed by LiTFSI solutions, particularly by LiTFSI·7H_2O, when modulated by spatial size and the presence of hydrophilic pore walls. It is noteworthy that these behaviors are distinct from those observed in LiFSI solutions under identical confinement conditions. Thus, these findings underscore the anion type-dependent modulating of confinement size and solid pore wall on the interactions between different components in confined Li salt solutions.

2. Experimental details

In this work, porous glass in disk form (Vycor 7930, Dow Corning Ltd.) with an average pore diameter of approximately 6.9 nm and an inner surface area of 130 m^2/g was employed. Among the numerous mesoporous and microporous materials currently available, Vycor glass is the only non-powder material. This material can effectively eliminate the influence of residual bulk liquids outside of pores or on the sample surface on the measured properties and structure of confined liquids. To eliminate the potential impact of organic molecules adsorbed onto the pore wall, Vycor glasses were subjected to a series of treatments. Specifically, they were soaked in H_2O_2 (30 wt%) at 363 K for 2 hours with ultrasound applied several times, and then continuously dried for 8 hours using nitrogen gas flow. LiTFSI and LiCl (99.9 wt%) were procured from Sigma, while LiFSI (99.9 wt%) was obtained from DoDo Chem. Different lithium salt aqueous solutions were created by dissolving the appropriate amount of salts in ultra-pure water (Millipore water, 18 MΩ·cm) and allowing them to stir for approximately 3 hours. The porous glass samples were then soaked in the solutions and stirred slowly for approximately 24 hours, and then were carefully dried with tissue paper and weighed before and after filling the target salt solution into the pores.

To monitor the vitrification process, a DSC PE8000 calorimeter was utilized with a scanning rate of 50 K/min, while each sample was hermetically sealed in an aluminum crucible. After cooling down to 133 K, the sample was held for 1 minute before the heating procedure commenced. The determination of T_g was done by following the conventional procedure adopted in previous studies.[27]

3. Results and discussion

To better understand the glass transition behavior of confined aqueous solutions of LiTFSI and even LiFSI, it is important to first provide a brief introduction to the characterization of bulk LiTFSI solutions. Our research group has recently developed a new state-diagram for this purpose.[28,29] Unlike a traditional phase diagram, which describes the equilibrium state of matter during a slow heating process, the state-diagram plots the concentration-dependent T_g of solutions and of the freeze-concentrated phase in water-rich solutions. Here, the term 'freeze-concentrated phase' typically denotes the liquid phase that experiences a concentration increase as a result of the crystallization of ice when cooling dilute aqueous solutions. This state diagram provides a universal division of solutions into three concentration zones, which is crucial for the discussion in this work. By understanding this division and its implications, we can then move on to examine the glass transition behavior of confined aqueous solutions of LiTFSI and LiFSI.

With the help of this new state diagram, the hydration number n_H of LiTFSI can be accurately quantified as $n_H = 7$.[29] This means that, in a water-rich solution, the solute together with water at a molar ratio of 1:7 can easily vitrify even under moderate and slow cooling rates. Considering the difficulty of bulk water vitrification, the number of these easily vitrified water is reasonably defined as n_H. Furthermore, the LiTFSI·$n$$H_2O$ system can be divided into three concentration zones: zone III for $n > 2.5n_H$, zone II for $2.5n_H > n > n_H$, and zone I for $n_H > n$. Normally, solutions within zone I only vitrify on cooling or devitrify upon heating processes, while solutions within zone II vitrify upon cooling and devitrify upon heating, but followed by cold-crystallization of ice.

Solutions within zone III will experience ice crystallization followed by the vitrification of the freeze-concentrated phase during the cooling process. Notably, the width of zone II for LiTFSI·$n$$H_2O$ is significantly larger than that of LiFSI $(2n_H > n > n_H)$ and other electrolytes with simple anions $(1.7n_H > n > n_H)$. This difference indicates that, compared to FSI^- and Cl^-, $TFSI^-$ causes a critical concentration point to shift towards the water-rich side. Above this critical solute concentration point, all water molecules can vitrify entirely under moderate cooling rates (*e.g.*, 1 K/min–20 K/min.). Below this threshold concentration point, only solute together bound water, $M \cdot n_H H_2O$, where M refers to the solute, can vitrify during the cooling process, while all other free water retains a bulk-like state and crystallizes into ice.

Another exceptional characteristic of LiTFSI·$n$$H_2O$ is the antiplasticizing effect of water observed in zone II.[29] Normally, T_g of bulk water is lower than that of solutes or concentrated solutions. Therefore, adding water to concentrated solutions would lower T_g of the system, as demonstrated for LiCl solutions (Fig. 2(f)). However, in contrast to LiFSI and other simple Li salt solutions, T_g of LiTFSI·$n$$H_2O$ increases as the water content increases within zone II (Fig. 1).

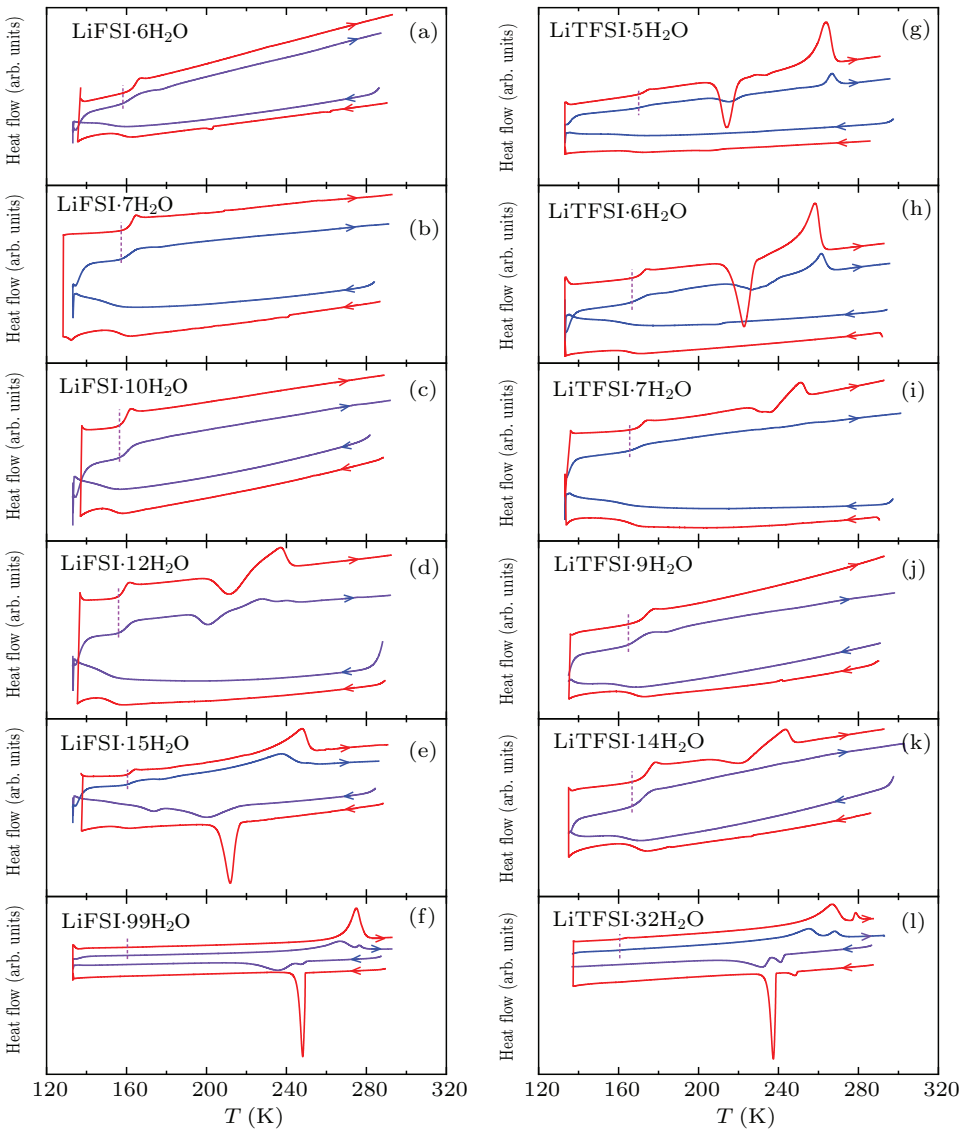


Fig. 1. The mass-normalized DSC cooling/heating curves of LiFSI·nH$_2$O [(a)–(f)] and LiTFSI·nH$_2$O [(g)–(l)] in the bulk state (red color) and when confined in averaged 6.9-nm-diameter silica-based pores with hydrophilic silanol group (blue color). For comparison purposes, dashed vertical lines indicate the location of the T_g of confined solutions. A cooling/heating rate of 50 K/min was used.

All these distinguishable characteristics of bulk LiTFSI solutions can still be observed in the confined state, as demonstrated in Figs. 1 and 2. At the same time, confined LiTFSI solutions additionally exhibit some special water content-dependent T_g. As a reference, LiCl solutions vitrify at a deeper supercooled state and experience almost negligible changes in T_g when confined in nanopores (Fig. 2(f)), as reported by Corti *et al.*[19] However, for LiFSI solutions in zones I and II, confinement significantly decreases T_g at LiFSI·4.5H$_2$O. This effect gradually weakens as water content increases and ultimately disappears at LiFSI·13H$_2$O (see Fig. 2(f)).

However, within zones I and II, LiTFSI·nH$_2$O shows a significantly different water content-dependent confinement effect on glass transitions, as evidenced in Fig. 2(e). The degree of confinement-induced reduction in T_g is negligible at LiTFSI·3.4H$_2$O and increases progressively, peaking at LiTFSI·9H$_2$O (Figs. 2(e) and 3), where $\Delta T_g = T_g(\text{confined}) - T_g(\text{bulk})$ is -5.98 K. Notably, at this concentration point, the water content-dependent T_g of confined LiTFSI·nH$_2$O also exhibits a minimum. Clearly, the concentration point, at which T_g exhibits a minimum, shifts from LiTFSI·7H$_2$O in the bulk state to LiTFSI·9H$_2$O when confined in nanopores. This behavior can be explained by the stronger tendency of some water molecules to preferentially coordinate with the silanol groups on the pore wall, as proposed by Elamin *et al.*[14]

Within zone III, bulk-like free water molecules crystallize into ice during the cooling process as seen in Figs. 1(e) and 1(f) for LiFSI solutions or Fig. 1(l) for LiTFSI·32H$_2$O, for example. This process is followed by the vitrification of freeze-concentrated phases such as LiFSI·7H$_2$O or LiTFSI·7H$_2$O between the pore wall and ice core. Importantly, this newly formed spatial confinement, referred to as "secondary confinement" herein for brevity, provides a means to control the thickness of the liquid film within a fixed pore diameter. The more water inside the pore, the greater the amount of ice crystallization during the cooling process. As a result, the liquid film between the ice core and the pore wall becomes thinner.

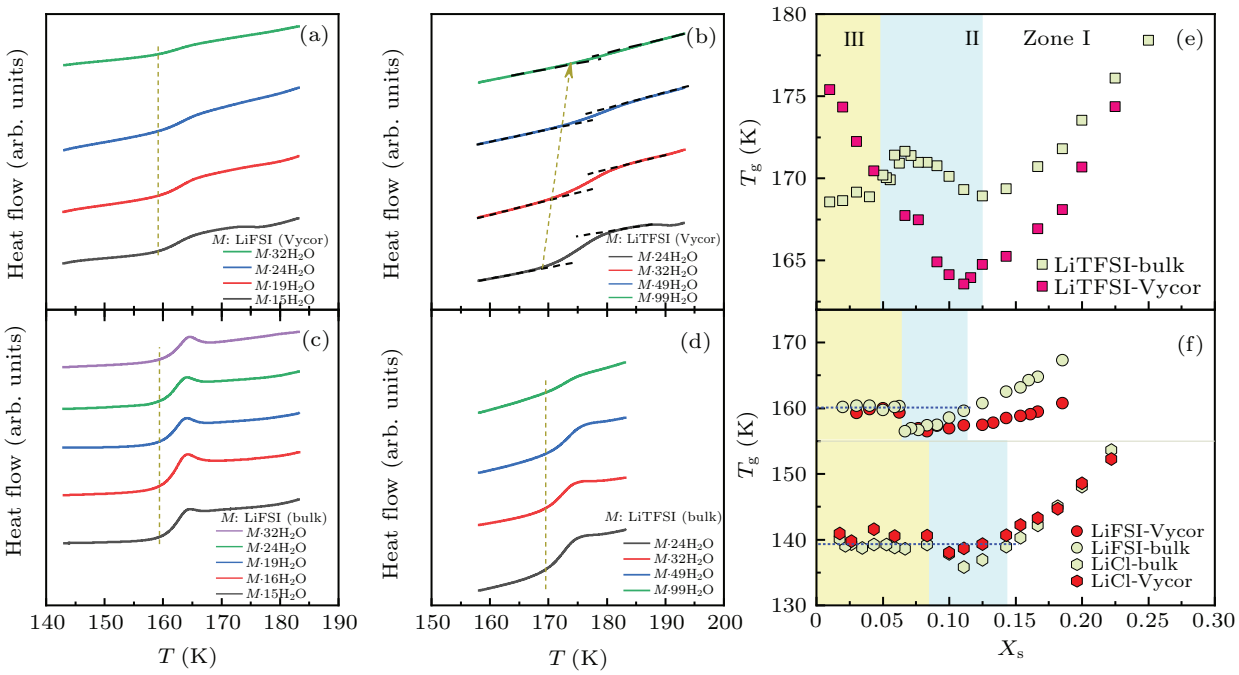


Fig. 2. Water content-dependent glass transition of the freeze-concentrated phase confined between pore wall and ice core for LiFSI solutions (a) and LiTFSI solution (b) compared with those in the bulk state [(c), (d)].

Under these conditions, the role of walls (or interface) and their hydrophilic/hydrophobic properties in affecting the dynamic properties of liquid can be effectively highlighted. For example, within zone III, as the freeze-concentrated phases of LiFSI·nH$_2$O and LiCl·nH$_2$O, respectively, LiFSI·7H$_2$O and LiCl·6H$_2$O keep almost constant T_g with increasing water content and then the thinning of the liquid layer between pore wall and core ice (Fig. 2(f) and Fig. 3). However, the freeze-concentrated phase of LiTFSI·nH$_2$O exhibits an obvious increase in T_g with decreasing thickness (Fig. 2(e); for further details, see Figs. 2(b) and (d)).

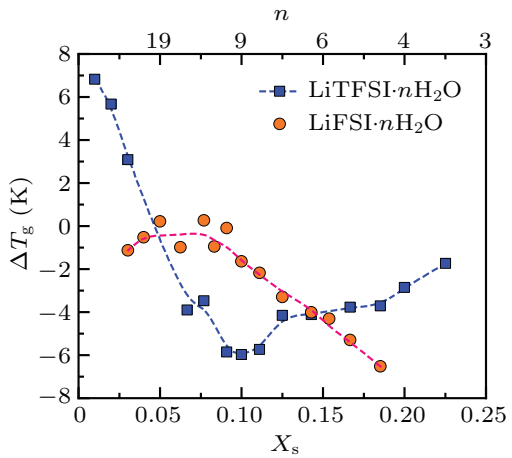


Fig. 3. Concentration-dependent the glass transition temperature of LiFSI solutions (red circles) and LiTFSI solutions (blue squares) when confined within Vycor porous glass.

The influence of confinement on the glass transition comes from two opposite effects: a decreasing pore size will reduce T_g especially when the pore size becomes comparable to the length scale of the dynamics of deeply supercooled solutions, and an increasing of the fraction of interfacial solutions, strongly affected by the presence of pore wall, will result in an increment in T_g.[20] Water molecules preferably hydrate with the hydrophilic silanol surface groups of the porous silica, leaving the majority of the glycerol molecules clustered in the center of the pores.[15] This proposition was adopted to explain a nearly constant T_g of glycerol solutions in MCM-41 for water concentrations between 0 and 85 wt%. This preferable interaction was also attributed to the factor resulting in the nanosegregation of confined glycerol solution with solute concentration below the eutectic composition.[20] The similar effect was highlighted in a study where a 1-nm-diameter BN nanotube, acting as a negative electrode, altered the interactions between different components of the 5-mol/kg LiTFSI solution.[10] The tube facilitated the dehydration of $TFSI^-$ ions and its subsequent preferential filling. The confinement between the pore wall and ice core can induce the vitrification of eutectic phase of NaCl solutions.[16] For the solutions with relatively weaker cation-water interaction, *i.e.*, for K^+, this confinement-induced vitrification behavior disappears. These examples emphasize the complexity of how surface and nanometer size affect the interactions between cations, anions and water.

In zone III, subsequent to the precipitation of crystallized ice, it has been noted that there is a marked difference in the relation between T_g and the thickness of the liquid film confined between the pore wall and ice core for LiFSI·7H$_2$O and LiTFSI·7H$_2$O. This observation indicates that the presence of a hydrophilic surface has a huge impact on the interactions among $TFSI^-$, Li^+, water, and/or the system-pore wall for LiTFSI·7H$_2$O in a manner that is significantly different from that observed for LiFSI·7H$_2$O, particularly within nanometer-

sized spatial spaces. This highlights the anion type-dependent confinement effect on the dynamic behaviors, particularly the relaxation process of deeply supercooled liquids, and ultimately their glass transitions.

4. Conclusion and perspectives

In summary, this study investigates the glass transition processes of LiTFSI·nH$_2$O, LiFSI·nH$_2$O, and LiCl·nH$_2$O, both in bulk and confined conditions, across a broad concentration range. Results show that in the absence of crystallized ice precipitation during cooling, the glass transition of these three solutions is influenced differently by the water content of confined spaces. LiCl·nH$_2$O shows almost no change in the glass transition temperature when confined in a 6.9-nm-diameter silica-based pore at all measured concentrations. For LiFSI·nH$_2$O, the confinement-induced reduction in the glass transition temperature is significant at LiFSI·4.4H$_2$O, but weakens monotonously with increasing water content, finally disappearing at LiFSI·17H$_2$O. In contrast, the confinement reduction effect on the glass transition temperature of LiTFSI·nH$_2$O is slight at LiTFSI·3.4H$_2$O but becomes more apparent as the water content increases, peaking at LiTFSI·9H$_2$O.

Moreover, importantly, when cooling water-rich solutions, the crystallization of water molecules induces a new confinement between pore wall and ice core. The thickness of liquid film within this secondary confinement will decrease with increasing water content. As a result, the influence of pore wall or solid/liquid interface on the relaxation dynamics of confined liquids should be effectively highlighted. We observed that, as the liquid film thickness decreases, LiFSI·7H$_2$O keeps almost constant glass transition temperature, and the glass transition temperature of LiTFSI·7H$_2$O monotonously increases. This different thickness-dependent glass transition temperature highlights a strong modulation of the presence of hydrophilic pore wall on the interactions between different components in LiTFSI·nH$_2$O.

As a prominent lithium salt in the "water in salt" system, LiTFSI has gained increasing popularity in low temperature applications.[30–32] In order to optimize its electrolyte performance and enhance its functionality in low temperature environments, it is crucial to gain a deep understanding of its low-temperature physicochemical and thermodynamic properties. Our study presents a promising approach to this point.

Acknowledgement

Project supported by the National Natural Science Foundation of China (Grant Nos. 11974385 and 91956101).

References

[1] Suo L M, Hu Y S, Li H, Armand M and Chen L Q 2013 *Nat. Commun.* **4** 1481
[2] Suo L, Borodin O, Gao T, Olguin M, Ho J, Fan X, Luo C, Wang C and Xu K 2015 *Science* **350** 938
[3] Lim J, Park K, Lee H, Kim J, Kwak K and Cho M 2018 *J. Am. Chem. Soc.* **140** 15661
[4] Yamada Y, Wang J, Ko S, Watanabe E and Yamada A 2019 *Nat. Energy* **4** 269
[5] Borodin O, Self J, Persson K A, Wang C and Xu K 2020 *Joule* **4** 69
[6] Li M, Wang C S, Chen Z W, Xu K and Lu J 2020 *Chem. Rev.* **120** 6783
[7] Cresce A and Xu K 2021 *Carbon Energy* **3** 721
[8] Meng Y S, Srinivasan V and Xu K 2022 *Science* **378** 1065
[9] Wang Y, Hao X, Kang Y, Dong M, Fang Z, Hu Y, Wang H, Fan X, Yan Y, Ye Z and Peng X 2023 *J. Mater. Chem. A* **11** 1394
[10] Chava B S, Wang Y, Sivasankar V S and Das S 2020 *Cell Reports Physical Science* **1** 100246
[11] Cheng C, Jiang G P, Simon G P, Liu J Z and Li D 2018 *Nat. Nanotech.* **13** 685
[12] Aydin F, Moradzadeh A, Bilodeau C L, Lau E Y, Schwegler E, Aluru N R and Pham T A 2021 *J. Chem. Theory Comput.* **17** 1596
[13] Hofer K, Mayer E and Johari G P 1991 *J. Phys. Chem.* **95** 7100
[14] Elamin K, Jansson H, Kittaka S and Swenson J 2013 *Phys. Chem. Chem. Phys.* **15** 18437
[15] Elamin K, Bjorklund J, Nyhlen F, Yttergren M, Martensson L and Swenson J 2014 *J. Chem. Phys.* **141** 034505
[16] Zhao L, Pan L, Cao Z and Wang Q 2016 *Chem. Phys. Lett.* **647** 170
[17] Swenson J, Elamin K, Chen G, Lohstroh W and Sakai V G 2014 *J. Chem. Phys.* **141** 214501
[18] Swenson J, Elamin K, Jansson H and Kittaka S 2013 *Chem. Phys.* **424** 20
[19] Longinotti M P, Fuentes-Landete V, Loerting T and Corti H R 2019 *J. Chem. Phys.* **151** 064509
[20] Angarita I, Mazzobre M F, Corti H R and Longinotti M P 2021 *Phys. Chem. Chem. Phys.* **23** 17018
[21] Corti H R, Appignanesi G A, Barbosa M C, Bordin J R, Calero C, Camisasca G, Elola M D, Franzese G, Gallo P, Hassanali A, Huang K, Laria D, Menendez C A, de Oca J M M, Longinotti M P, Rodriguez J, Rovere M, Scherlis D and Szleifer I 2021 *Eur. Phys. J. E* **44** 136
[22] Alcoutlabi M and McKenna G B 2005 *J. Phys.: Condens. Matter* **17** R461
[23] Jackson C L and McKenna G B 1991 *J. Non Cryst. Solids* **131–133** 221
[24] Priestley R D, Ellison C J, Broadbelt L J and Torkelson J M 2005 *Science* **309** 456
[25] Wang L M, He F and Richert R 2004 *Phys. Rev. Lett.* **92** 095701
[26] Royall C P and Williams S R 2015 *Phys. Rep.* **560** 1
[27] Zhao L S, Cao Z X and Wang Q 2015 *Sci. Rep.* **5** 15714
[28] Zhao L S, Pan L Q, Cao Z X and Wang Q 2016 *J. Phys. Chem. B* **120** 13112
[29] Zhang J, Wang F, Cao Z and Wang Q 2021 *J. Phys. Chem. B* **125** 13041
[30] Li C C, Zhang S Y, Wang Y F, Liu H Y, Xing T, Lin Y, Rong X C, Ren H, Wu M B, Abbas Q and Li Z T 2022 *J. Power Sources* **544** 231874
[31] Reber D, Kühnel R S and Battaglia C 2019 *ACS Materials Lett.* **1** 44
[32] Yue J, Zhang J, Tong Y, Chen M, Liu L, Jiang L, Lv T, Hu Y S, Li H and Huang X 2021 *Nat. Chem.* **13** 1061